

Image Cover Sheet

CLASSIFICATION

UNCLASSIFIED

SYSTEM NUMBER

513096



TITLE

Analysis of Reverse Dive Profiles Using the DCIEM Bubble Evolution Model. Part
2: Risk Assessment

System Number:

Patron Number:

Requester:

Notes:

DSIS Use only:

Deliver to:



ANALYSIS OF REVERSE DIVE PROFILES USING THE DCIEM BUBBLE EVOLUTION MODEL PART II. RISK ASSESSMENT

Ron Y. Nishi
Peter Tikuisis

Defence and Civil Institute of Environmental Medicine
1133 Sheppard Avenue West, PO Box 2000
Toronto, ONTARIO M3M 3B9 CANADA

The DCIEM Bubble Evolution Model was used for a risk assessment analysis of a number of real and computed reverse and conventional repetitive dive profiles. The results suggest ways of managing and reducing the risk of reverse dive profiles.

Introduction

The DCIEM Bubble Evolution Model is a probabilistic model that has been calibrated with observed levels of venous gas emboli detected with the Doppler ultrasonic bubble monitor. It is used to calculate the growth and decay of bubbles generated by a dive/decompression profile. The predicted maximum bubble radius (max BR) attained can be used as a measure of the risk of decompression sickness (DCS). The model will be used to look at a number of calculated and real dive profiles to determine if reverse dive profiles are inherently more risky than normal repetitive dive profiles, which consist of a deeper dive followed by a shallower dive.

Repetitive Dive Models

In any analysis of repetitive dives, it is important to consider what was used to calculate the repetitive requirements. Calculation of repetitive dives either by means of tables or dive computers depends on the "decompression model" (or, more correctly, decompression algorithm) that was used to generate the tables or that is embodied within the dive computers.

There are two types of models for calculating repetitive dives. Ideally, the "decompression model" or dive computer should base the requirements of the repetitive dive on a continuous monitoring of all the compartment pressures. Figure 1 shows an example of repetitive dives being done with such a dive computer (Kidd and Stubbs, 1969). These types of dives were used to test and develop the Kidd-Stubbs "decompression model," the precursor of the present-day DCIEM model.

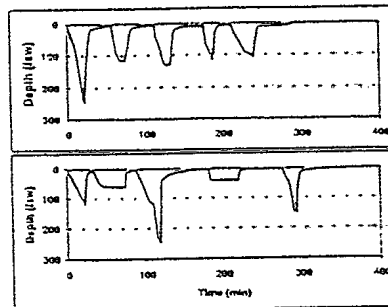


Figure 1. Examples of dives used to test original DCIEM model (Kidd-Stubbs, 1964-1969).

The other type of model is the Haldane/Workman/Schreiner (H/W/S) model that is the basis of most of the tables and dive computers that are available. This model uses a Residual Nitrogen Time (RNT) concept by looking at the compartment pressure in the 120 min half-time compartment, for

example, in the case of the U.S. Navy decompression tables and in the 60 min half-time compartment in the case of the PADI/DSAT Recreational Dive Planner (Hamilton *et al.*, 1994). The RNT model has severe limitations and will give completely different results under certain conditions. Attempting to use the H/W/S model directly to compute repetitive dive requirements by monitoring the pressure values in all compartments generally results in very liberal repetitive dive times, and it is necessary to make numerous adjustments and modifications to the model to obtain safe repetitive dives (Hamilton, 1995).

Analysis of Real Dive Data with the Bubble Model

One of the first major applications of the bubble model was for the analysis of multiple repetitive dive profiles that were being conducted by the pearl divers of Western Australia (Wong, 1996). Figure 2 shows a typical daily routine: 10 repetitive dives a day for 8 continuous days. The depth for each excursion is 19 msw with a bottom time of 40 minutes, with some decompression stops on oxygen at 9 msw. The original profiles were empirical dives that had been developed over the years.

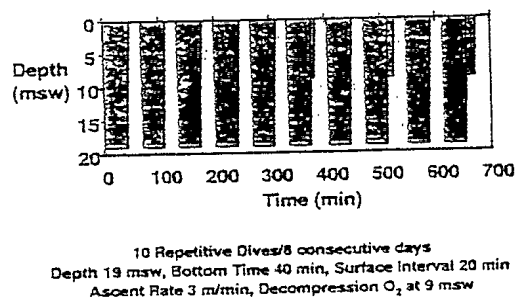


Figure 2. Pearl divers' multiple repetitive dive schedule

Figure 3 shows a more typical "at sea" operational dive and shows that some of the pearl diving involves reverse dives. This is not necessarily a result of the diver moving into deeper water. It is caused by tidal variations. The tides in northwestern Australia are among the greatest in the world, and there could be a change as great as 9 metres. Also shown in the figure are the calculated bubble evolution curves for both the first and second compartments in the model.

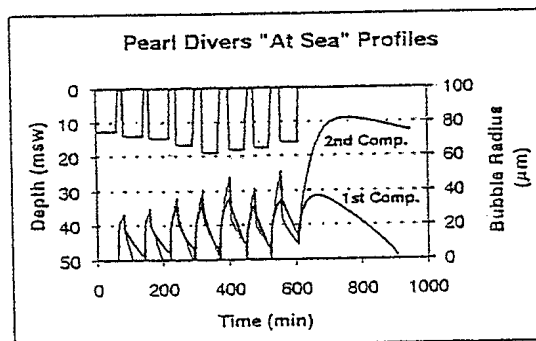


Figure 3. Calculated bubble evolution for multiple repetitive dives

An analysis of this particular series of dives shows that bubbles are generated during the surface interval between each dive, then redissolve and collapse during the next dive, form again and so on. During the surface interval, the growth is limited because of the short surface interval that helps explain the inherent safety of such procedures. Mike Gernhardt has used this concept of limiting the bubble growth to develop successful surface decompression tables with his Bubble Growth Index Model (Gernhardt, 1991). The most dangerous part of the dive is at the end, because the final bubble can grow considerably and it is important to provide sufficient decompression at the end.

Figure 4 shows the results obtained from a series of dive profiles from 11 to 23 metres depth that were tested in a hyperbaric chamber by Dr. Robert Wong, medical consultant to the pearl diving

industry. The purpose of these dives was to evaluate the dive schedules that were being used in the industry and to determine how they could be improved by implementing additional decompression stops on oxygen. The DCIEM air diving model was used to determine the decompression requirements. The results (Nishi, 1999) show that for those profiles where the max BR at the end of the dives were greater than 70 μm , DCS always seemed to occur. High bubble levels, Doppler Grades 3 and 4, occurred at 60 μm or greater and below that, low bubble grades were observed. Grade 3 and 4 bubbles are associated with high decompression stress and an increased risk of DCS (Nishi, 1993). These results give us a good idea as to what to expect when analyzing repetitive dives. A good guideline for this type of diving would appear to be to keep the max BR produced by any dive profile below 60 μm . However, a potential problem with these predictions might arise with acclimatization since the pearl divers conduct many dives per day for 8 consecutive days.

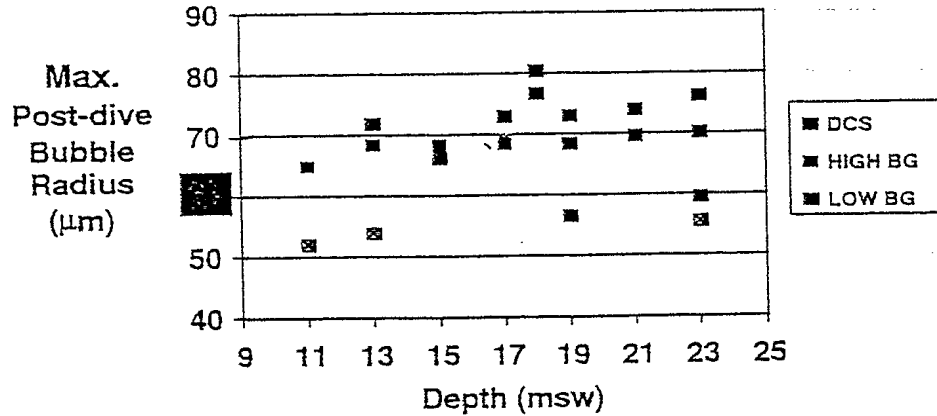


Figure 4. DCS bubble radius threshold for pearl divers' profiles (1992-1997).

Figure 5 shows another example from the pearl diving industry that shows multiple repetitive dives demonstrating both shallow subsequent dives and also increasingly deeper repetitive dives. There are a few interesting features. Normally, we think of a longer surface interval between dives as being safer than shorter surface intervals. However, in a case like this where there is a large gas loading, a longer surface interval such as observed after the fifth dive allows the bubble to grow considerably before the next dive begins and can put the diver at risk of DCS.

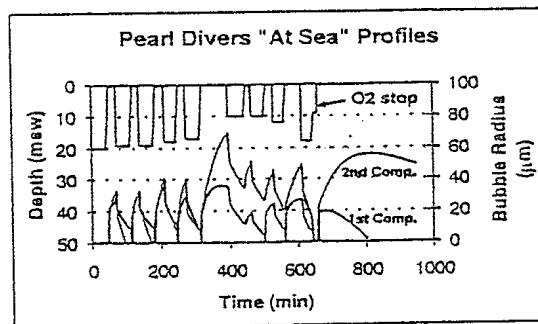


Figure 5. Calculated bubble evolution for multiple repetitive dives.

It is also interesting to note that a deep dive followed by a shallow dive may not be sufficient to cause the bubbles generated by the previous dive to redissolve and collapse and may lead to larger bubbles being formed during the next surface interval. Finally, it can be seen that providing more decompression for the last dive, either by giving oxygen or more decompression time can reduce the maximum bubble size and bring it down to a lower risk range.

One of the handicaps in developing decompression models and relating them to real dive and DCS information is the difficulty in obtaining large quantities of DCS data to accurately define the model. Recent work by the U.S. Navy and Dr. Charles Lehner at the University of Wisconsin (Lehner *et al.*, 1997) using probabilistic modeling has shown that sheep appear to be a good analogue for human diving (Ball *et al.*, 1999). The sheep data set is for single dives and comprises a considerable number of DCS cases.

Figure 6 shows observed DCS incidence versus max BR for part of this data set in two pressure ranges. For pressures in the range of 50 to 100 fsw, DCS occurred at around 60 μm and, as the bubble size increased, more and more subjects were observed to have DCS. This is consistent with the results shown in Part I. However, for depths greater than 100 fsw and less than 140 fsw, DCS occurred at a lower max BR, starting at about 45 μm . In addition, the observed DCS incidence increased more rapidly with increasing bubble size. So for non-acclimatized subjects, the threshold between low risk and high risk should perhaps be set at around 40 μm for reverse dives. For the shallower depths, the threshold could possibly be set at a higher value.

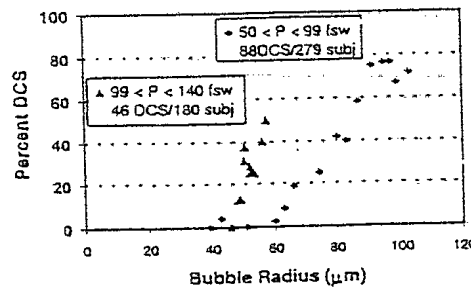


Figure 6. Percent observed DCS versus BR – Sheep Large Animal Model (Lehner et al., 1997)

Using the Bubble Model for Prediction of Risk

Tables 1 and 2 show the results of no-decompression limit (NDL) predictions for the DCIEM model and tables, the PADI/DSAT H/W/S model and tables, and the USN H/W/S model and tables. Both the PADI and USN H/W/S models were used directly as designed for first dives and no adjustments or modifications were made to the half-times or M-values. The dive conditions were 40 and 60 fsw to the NDL followed by a second dive to the NDL at 100 fsw after several different surface intervals, and a first dive of 100 fsw to the NDL followed by second dives at the NDL for 40 and 60 fsw.

Table 1. Calculated NDL's and Maximum Bubble Radii for Normal and Reverse Dive Profiles at 40 fsw and 100 fsw.

1st Dive	SI	2nd Dive	2nd Dive Bottom Time for different models												
			dciem				dsat				usn.air				
			Depth	model	table	BR	Depth	model	table	BR	Depth	model	table	BR	
40	30	0.5	100	10	32.2	10	31.8	18	40.8	12	34.1	22	44.9	11	32.8
40	30	1.0	100	11	31.2	11	30.8	19	39.4	14	34.5	23	43.0	11	30.8
40	30	2.0	100	12	30.9	11	29.8	19	38.7	17	36.7	23	42.2	15	34.5
40	30	4.0	100	12	30.9	13	32.0	19	38.5	17	36.4	23	42.0	22	41.1
40	60	0.5	100	9	38.5	9	38.3	18	49.5	6	33.9	21	53.2	n/a	
40	60	1.0	100	11	36.6	9	34.7	19	47.2	11	37.2	23	51.5	3	27.9
40	60	2.0	100	11	31.7	10	30.0	19	41.8	14	35.6	23	46.9	11	31.3
40	60	4.0	100	12	30.6	11	29.2	19	38.5	17	36.4	23	42.1	15	34.3
40	90	0.5	100	8	46.7	7	43.1	16	53.3	2	42.0	19	57.9	n/a	
40	90	1.0	100	10	43.4	8	42.1	19	54.0	8	42.1	23	57.8	n/a	
40	90	2.0	100	11	38.7	9	38.5	19	48.7	14	41.8	23	52.3	3	39.2
40	90	4.0	100	12	30.2	10	28.4	19	40.1	17	37.6	23	45.2	15	34.4
40	120	0.5	100	8	52.9	n/a		14	59.1	n/a		18	62.3	n/a	
40	120	1.0	100	9	52.7	7	52.2	19	59.1	6	52.0	23	62.7	n/a	
40	120	2.0	100	11	50.2	8	49.8	19	53.4	12	50.4	23	57.2	n/a	
40	120	4.0	100	11	39.6	9	39.6	19	45.5	17	42.6	23	49.8	11	39.5
40	150	0.5	100	7	59.7	n/a		12	61.9	n/a		17	65.7	n/a	
40	150	1.0	100	9	59.8	n/a		19	63.3	5	59.0	23	66.9	n/a	
40	150	2.0	100	10	57.9	7	57.3	19	59.8	12	58.2	23	61.3	n/a	
40	150	4.0	100	11	49.1	9	48.9	19	50.6	17	50.7	23	54.2	11	49.0
100	10	0.5	40	125	57.6	115	55.6	123	57.2	118	56.3	179	65.9	163	64.0
100	10	1.0	40	128	57.4	125	56.8	128	57.5	124	56.6	184	66.0	163	63.4
100	10	2.0	40	133	57.2	125	55.6	135	57.6	131	56.9	190	66.3	175	64.2
100	10	4.0	40	138	56.9	136	56.5	139	57.2	131	55.5	196	65.8	193	65.5
100	15	0.5	40	112	57.3	100	54.9	113	57.5	109	56.7	168	66.0	151	63.9
100	15	1.0	40	118	57.2	107	55.0	122	58.0	118	57.2	176	66.4	163	64.6
100	15	2.0	40	124	56.7	115	54.8	132	58.2	131	58.0	186	66.5	175	65.0
100	15	4.0	40	133	56.3	125	54.8	139	57.5	131	56.0	194	66.2	183	64.6
100	20	0.5	40	n/a	n/a			102	57.9	100		157	66.4	139	64.0
100	20	1.0	40	n/a	n/a			116	58.9	113		168	66.7	151	64.5
100	20	2.0	40	n/a	n/a			129	59.1	124		181	66.9	163	64.5
100	20	4.0	40	n/a	n/a			136	58.3	131	56.9	193	66.5	183	65.2
100	25	0.5	40	n/a	n/a			n/a	n/a			145	66.5	113	62.1
100	25	1.0	40	n/a	n/a			n/a	n/a			160	67.0	127	62.6
100	25	2.0	40	n/a	n/a			n/a	n/a			177	67.3	151	63.9
100	25	4.0	40	n/a	n/a			n/a	n/a			191	66.9	175	64.8

Table 2. Calculated NDL's and Maximum Bubble Radii for Normal and Reverse Dive Profiles at 60 fsw and 100 fsw.

1st Dive		SI	2nd Dive		2nd Dive Bottom Time for different models											
Depth ft	BT min		Depth ft	dciem				dsaf				usn.ar				
				model	table	model	table	model	table	model	table					
60	30	0.5	100	9	35.3	9	35.3	18	45.3	8	34.9	22	49.8	3	33.14	
60	30	1.0	100	11	33.3	9	32.7	19	43.1	12	33.9	23	48.0	7	27.9	
60	30	2.0	100	12	30.9	10	28.8	19	39.1	14	34.0	23	43.3	11	30.32	
60	30	4.0	100	12	30.7	11	29.2	19	38.5	17	36.5	23	42.1	18	37.34	
60	40	0.5	100	8	39.1	8	38.7	17	49.1	4	37.2	20	52.5	n/a		
60	40	1.0	100	10	37.5	9	31.0	19	48.4	9	36.7	23	52.5	3	34.67	
60	40	2.0	100	11	32.6	10	31.0	19	42.9	14	36.7	23	47.8	11	32.27	
60	40	4.0	100	12	30.6	11	29.7	19	38.6	17	36.5	23	40.9	15	34.37	
60	50	0.5	100	8	43.7	8	43.9	15	52.1	2	39.4	18	55.2	n/a		
60	50	1.0	100	10	41.6	8	39.4	19	53.3	7	39.0	23	56.5	n/a		
60	50	2.0	100	11	36.7	9	35.2	19	46.9	14	40.4	23	51.1	7	35.3	
60	50	4.0	100	12	30.8	10	28.3	19	38.9	17	36.5	23	43.7	15	34.44	
100	10	0.5	60	26	33.6	31	36.8	46	46.9	41	43.3	56	51.9	36	40.12	
100	10	1.0	60	29	33.4	35	37.8	50	47.8	44	43.5	60	52.6	36	38.44	
100	10	2.0	60	31	33.4	35	35.1	53	47.2	49	44.2	63	52.5	43	40.49	
100	10	4.0	60	32	33.5	40	36.5	54	45.2	49	41.6	65	51.2	49	41.57	
100	15	0.5	60	23	35.9	27	38.9	43	48.8	36	45.0	51	53.0	30	40.82	
100	15	1.0	60	27	36.1	29	37.6	49	50.0	41	45.7	57	54.5	36	42.14	
100	15	2.0	60	29	33.3	31	34.5	53	49.1	49	47.0	62	54.3	43	42.91	
100	15	4.0	60	31	33.3	35	34.9	54	46.2	49	42.7	65	52.0	49	42.66	
100	20	0.5	60	n/a	n/a			38	50.5	30		46	54.8	24	41.92	
100	20	1.0	60	n/a	n/a			47	52.4	38		55	56.4	30	42.59	
100	20	2.0	60	n/a	n/a			53	51.7	44		62	56.4	38	41.48	
100	20	4.0	60	n/a	n/a			54	47.9	49	44.5	65	53.8	49	44.49	
100	25	0.5	60	n/a	n/a			n/a	n/a	n/a		41	56.1	8	43.2	
100	25	1.0	60	n/a	n/a			n/a	n/a	n/a		52	58.2	16	41.27	
100	25	2.0	60	n/a	n/a			n/a	n/a	n/a		61	58.2	30	41.14	
100	25	4.0	60	n/a	n/a			n/a	n/a	n/a		65	55.4	43	42.89	

The NDL varies greatly depending on what model is being used. With a 120 min halftime RNT, the U.S. Navy tables do not allow a reverse dive profile for short surface intervals. The PADI tables, based on a 60 min RNT compartment, are more liberal and will allow dives that the USN will not. The DCIEM model, which does not work on RNT's, allows a greater bottom time for shorter surface intervals than the other two tables. However, it is a more conservative model for repetitive no-decompression dives and gives shorter NDL's than the other two tables for longer surface intervals. The DCIEM (1992) repetitive dive tables give longer NDL's because some adjustments have been made to approach the first dive no-decompression limits at long surface intervals. The H/W/S models give very liberal NDL's that quickly approach the first dive's NDL's.

The max BR calculated for these dives shows that for a reverse dive, the first dive should not be done at or close to the NDL, if we assume a 40 µm max BR as a threshold for high risk. If a reverse dive is planned, then in order to control the risk, it will be necessary to back off from the NDL for the first dive. For a reverse dive, the bottom time of the first dive is important.

On the other hand, a deep dive followed by a shallower dive shows a different response. All models and tables now predict that the second dive is possible. The 60 min halftime RNT gives more liberal NoD times. The DCIEM model is probably too conservative and does not allow much time for long surface intervals at 60 fsw. If we look at the maximum bubble radii, it is more consistent with our belief that longer bottom times will give greater risk. In this case, it may not be wise to select the table or computer that will give the longest bottom time on the second dive.

An interesting observation for reverse dives is that regardless of whether or not bottom time of the second dive is long or short, the calculated max BR does not vary greatly when the gas loading on the first dive is high. For example, a first dive of 40 fsw for 90 minutes and a second dive of 100 fsw after a 2 hr surface interval shows that regardless of whether the NDL is 3 minutes as in the USN predictions or 14 min as in the PADI predictions, the max BR is approximately the same. However, the time to reach max Br is different. Figure 7 shows the detailed bubble evolution for these dives. A short deep second dive that is only 3 minutes long is not sufficient to collapse the bubbles generated by the first dive, and, hence, the starting base for a gas bubble from the second dive is much higher than expected. On the other hand, a longer bottom time second dive gives the bubbles generated by the first dive the time to be compressed and dissolved away. In this particular case, both the 3 min USN dive and the 14 min PADI dive give about the same maximum bubble size.

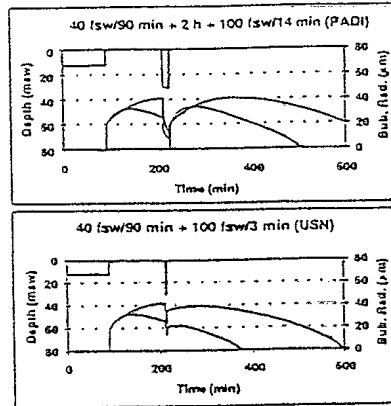


Figure 7. Comparison of short and longer deep dives.

This is not a problem peculiar to deep dives following a shallow dive. The same thing could happen with a short shallow dive following a long deep dive where the gas loading from the first dive can be substantial. Another factor comes into play for a shallow second dive. The depth of the second dive may not be sufficient to allow all the bubbles arising from the first dive to be dissolved away. Both of these conditions are illustrated in Figure 5.

Comparison of Predictions with Real Dive Data

During the development of the DCIEM air diving tables, two repetitive dive profiles, a normal deep first dive followed by a shallow second dive, and a reverse dive profile were tested. Figure 8 shows the normal repetitive dive sequence, a dive to 120 fsw for 10 min followed by a dive to 60 fsw for 38 minutes after 1 hour. The max BR after the dives was around 40 µm. This sequence resulted in a relatively moderate stress sequence with one of 17 subjects reporting Grade 3 bubbles. There were no cases of DCS.

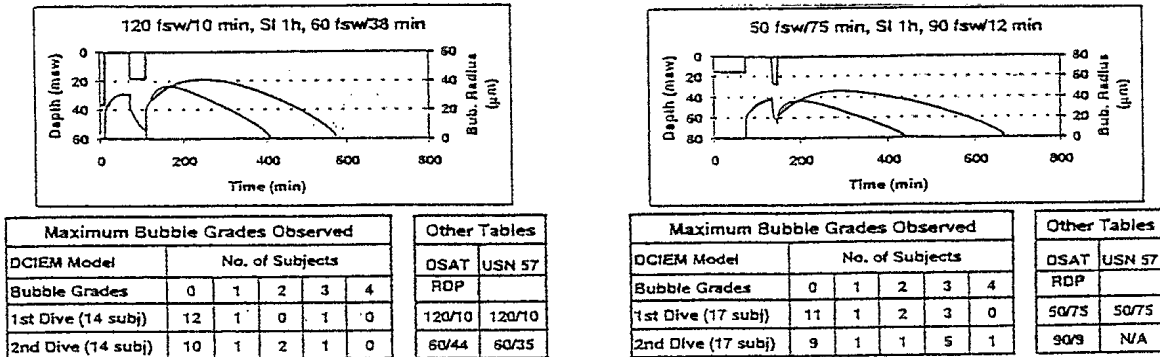


Figure 8. Results of experimental deep/shallow dive. Figure 9. Results of experimental shallow/deep dive.

Figure 9 shows a reverse dive profile, a dive to 50 fsw for 75 minutes followed by a 90 fsw dive for 12 minutes. The max BR after the second dive was around 45 µm. This was a somewhat more stressful dive with three divers on the first dive with Grade 3 bubbles and 5 divers on the second dive with Grade 3 bubbles, suggesting that the second dive was more stressful than the first. The PADI tables allowed only 9 minutes for the second dive and the USN tables did not allow a repetitive dive. Although this is a very limited comparison, it does suggest that the choice of 40 µm may be appropriate as the threshold between low-risk and high-risk repetitive dives.

A third example (Figure 10) has been taken from the PADI/Diving Science and Technology trials for the Recreational Dive Planner (Hamilton *et al.*, 1994). Phase II of the trials involved 6 dives a day for 6 days. Only the first day is shown here with the last three dives being reverse dive profiles. A similar

sequence was conducted on the second day and the third day of trials was discontinued because of a case of DCS. Of the six dives, the third to the sixth dives all resulted in max BR of greater than 40 μm . After all these dives, Grade 3 bubbles were reported in some of the subjects. So this is also consistent with dives that have a predicted max BR greater than 40 being of high decompression stress. More decompression would have been desirable for the last dive since the max BR was about 65 μm .

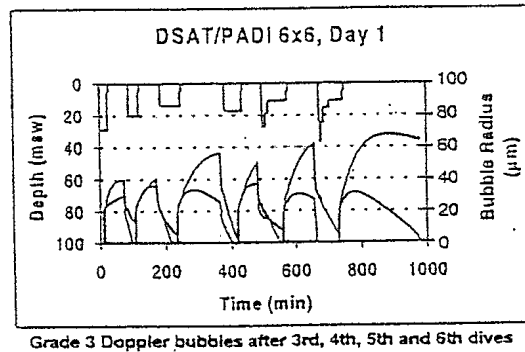


Figure 10. Bubble evolution for PADI experimental dives.

Summary

The risk of reverse dive profiles depends on what decompression algorithm is used to predict the second dive requirements. This same comment can be made for all repetitive dives, not only reverse dives. If reverse dive profiles are planned, it should be planned to dive conservatively, and the first dive should not be done at or near the NDL. An alternative would be to consider the use of oxygen decompression such as used by pearl divers. It should be kept in mind that there may be additional risks involved when doing a very short deep dive. However, this could also be true for a shallow dive following a deeper first dive.

In closing, analysis tools, like the bubble model described here, give us a more intuitive insight into the risks involved in reverse dives.

Literature Cited

- DCIEM. 1992. DCIEM Diving Manual: Part 1. Air Decompression Procedures and Tables. Universal Dive Techtronics, Richmond, BC, Canada.
- Gerrhardt, M.L. 1991. Development and evaluation of a decompression stress index based on tissue bubble dynamics, Ph.D. Thesis, University of Pennsylvania, Philadelphia, Pennsylvania.
- Hamilton, R.W., R.E. Rogers, M.R. Powell, and R.D. Vann. 1994. Development and validation of no-stop decompression procedures for recreational diving: The DSAT Recreational Dive Planner. Diving Science and Technology Corp.
- Hamilton, R.W. (ed.) 1995. The Effectiveness of Dive Computers in Repetitive Diving. UHMS 81(DC)6-1-94. Undersea and Hyperbaric Medical Society, Inc., Kensington, Maryland.
- Kidd, D.J. and R.A. Stubbs. 1969. The use of the pneumatic analog computer for divers. In: Bennett, P.B. and D.H. Elliott (eds.). The Physiology and Medicine of Diving and Compressed Air Work, 1st edition. Bailliere, Tindall and Cassell, London, pp. 386-413.
- Lehner, C.E., R. Ball, D.D. Gummin, E.H. Lanphier, E.V. Nordheim, and P.M. Crump. 1997. Large-animal model of human decompression sickness: sheep database and preliminary analysis. Naval Medical Research Institute Report NMRI 97-02, Bethesda, Maryland.

- Nishi, R.Y. 1993. Doppler and ultrasonic bubble detection. *In: Bennett, P.B. and D.H. Elliott (eds.). The Physiology and Medicine of Diving, 4th Edition, W.B. Saunders, London, Chapter 15, pp. 433-453.*
- Nishi, R.Y. (in press). Modeling the risk of DCS in empirical diving techniques. *Proceedings of the UHMS Workshop on Empirical Diving Techniques of Commercial Sea Harvesters, Richmond, British Columbia, 25-26 May 1998.*
- Wong, R.M. 1996. Doppler studies on the dive schedules of the pearl divers of Broome. *SPUMS Journal 26 (Suppl.), 36-48.*

513096